Journal of Medicinal Chemistry

Article

pubs.acs.org/jmc

Synthesis and Structure–Activity Relationships of New Quinolone-Type Molecules against *Trypanosoma brucei*

Georg Hiltensperger,[†] Nicola G. Jones,[‡] Sabine Niedermeier,[†] August Stich,[§] Marcel Kaiser,[∥,⊥] Jamin Jung,[‡] Sebastian Puhl,[†] Alexander Damme,[#] Holger Braunschweig,[#] Lorenz Meinel,[†] Markus Engstler,[‡] and Ulrike Holzgrabe*[,†]

[†]Institut für Pharmazie and Lebensmittelchemie, Universität Wuerzburg, Am Hubland, 97074 Würzburg, Germany

[‡]Department of Cell and Developmental Biology, Universität Wuerzburg, Am Hubland, 97074 Würzburg, Germany

[§]Medical Mission Institute, Salvatorstrasse 7, 97067 Würzburg, Germany

[∥]Swiss Tropical and Public Health Institute, Socinstrasse 57, 4051 Basel, Switzerland

[⊥]Swiss University of Basel, Petersplatz 1, 4051 Basel, Switzerland

[#]Institute of Inorganic Chemistry, Universität Wuerzburg, Am Hubland, 97074 Würzburg, Germany

Supporting Information

ABSTRACT: Human African trypanosomiasis (HAT) or sleeping sickness is caused by two subspecies of *Trypanosoma brucei*, *Trypanosoma brucei gambiense*, and *Trypanosoma brucei rhodesiense* and is one of Africa's old plagues. It causes a huge number of infections and cases of death per year because, apart from limited access to health services, only inefficient chemotherapy is available. Since it was reported that quinolones such as ciprofloxacin show antitrypanosomal activity, a novel quinolone-type library was synthesized and tested. The biological evaluation illustrated that 4-quinolones with a benzylamide function in position 3 and cyclic or acyclic amines in position 7 exhibit high antitrypanosomal activity. Structure–activity relationships (SAR) are established to identify essential structural elements. This analysis led to lead structure **29**, which exhibits promising in vitro activity against *T. b. brucei* (IC_{50} = 47 nM) and *T. b. rhodesiense* (IC_{50} = 9 nM) combined with low cytotoxicity against macrophages J774.1. Screening for morphological changes of trypanosomes treated with compounds **19** and **29** suggested differences in the morphology of mitochondria of treated cells compared to those of untreated cells. Segregation of the kinetoplast is hampered in trypanosomes treated with these compounds; however, topoisomerase II is probably not the main drug target.

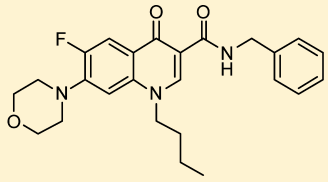

IC_{50} = 9 nM against the human pathogenic subspecies *Trypanosoma brucei rhodesiense*

INTRODUCTION

Human African trypanosomiasis (HAT), also known as sleeping sickness, is caused by infection with one of two subspecies of *Trypanosoma brucei*. *Trypanosoma brucei rhodesiense* is found in Eastern and Southern Africa, whereas *Trypanosoma brucei gambiense* occurs in Western and Central Africa and is responsible for over 90% of all reported cases of infection.[1]

In the last 120 years, Africa saw three severe sleeping sickness epidemics. In 1896, the first one mainly affected Uganda and Congo and caused approximately 500000 deaths.[2,3] The ensuing drug development, supported by colonial administrations, helped to combat the second severe outbreak in 1920.[2] Another important approach toward the containment of HAT was the elimination of the parasite reservoir so that within 11 years the prevalence of sleeping sickness decreased from 60% in some areas to 0.2–4.1%. By the mid 1960s, most of the endangered countries became independent. The upcoming political instability had a disastrous effect on the health services, furthermore, the control of HAT was no longer a priority and led to the third and most recent epidemic in the 20th century, mainly affecting the Democratic Republic of Congo, Angola, Southern Sudan, and Uganda.[4] In 1997, surveillance in sub-Saharan Africa had been reinforced. Current estimations show that about 60 million people are at risk in sub-Saharan Africa with 50000–70000 cases occurring annually.[5]

Both subspecies are transmitted by the bite of infected tsetse flies. *T. b. gambiense* HAT is primarily a chronic human disease. *T. b. rhodesiense* HAT is primarily zoonotic with a huge animal reservoir and causes the acute form of sleeping sickness. Both forms of HAT show two clinical stages. The first corresponds to the multiplication of the parasites in the blood and lymphatic system. After crossing the blood–brain barrier, the trypanosomes attack the central nervous system and neurological symptoms appear. Without medical treatment, coma and finally death results. The medical treatment is based on only five commercially available drugs: suramine and pentamidine are used in treatment of the first stage, and melarsoprol and eflornithine, which both are able to cross the blood–brain

Received: November 9, 2010
Published: March 1, 2012

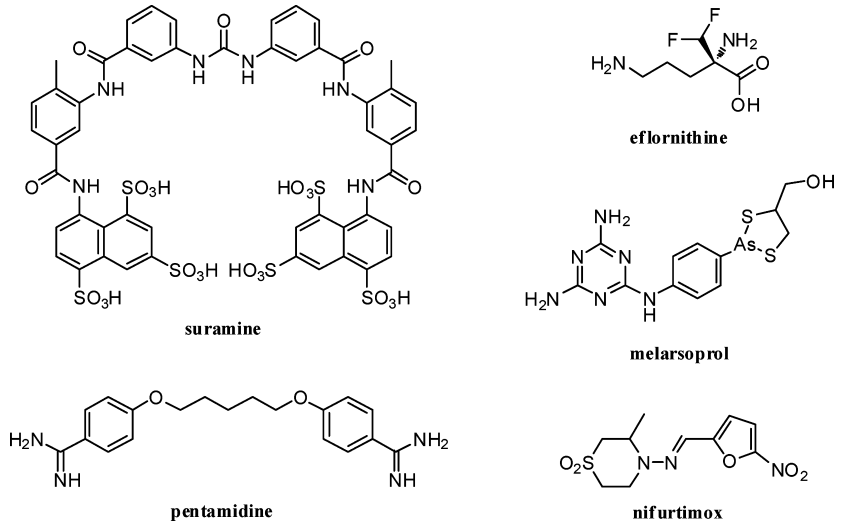

Figure 1. Structures of commercially available drugs.

barrier, are employed in the therapy of the second stage. A fifth drug, nifurtimox, was recently introduced as a partner in combination therapies for *T. b. gambiense* HAT (Figure 1).[6] All treatment regimens were established during the last 20 years, and some suffer from severe, sometimes life-threatening side-effects, e.g., melarsoprol as an arsenic containing drug, is lethal in 4−6% of treated patients. Moreover, drug resistance is spread to an extent that medical treatment of HAT is rapidly losing its effectiveness in many African regions.[7,8]

Consequently, new active compounds are urgently needed. Parasitic targets such as cytochrome-independent oxidase, fatty acid biosynthesis, and purine salvage provide a basis for new drug design.[7,9,10] Another interesting target is the kinetoplast DNA (kDNA) replication machinery in which the topoisomerase is responsible for the unique structure of kDNA.[11] Recently, it was reported that topoisomerase II inhibitors like nalidixic acid, ciprofloxacin, gatifloxacin, and moxifloxacin showed activity against the topoisomerases II of trypanosomes (Figure 2).[8,12] Even though structural variations mainly with regard to the basic heterocycles in position 7 and condensed rings (from N1 to C8 and N1 to C2) were performed, the antitrypanosomal activity stayed in the low micromolar range. Furthermore, ciprofloxacin derivatives exhibited antitrypanosomal potency but seemed to lack in vivo activity.[13−16]

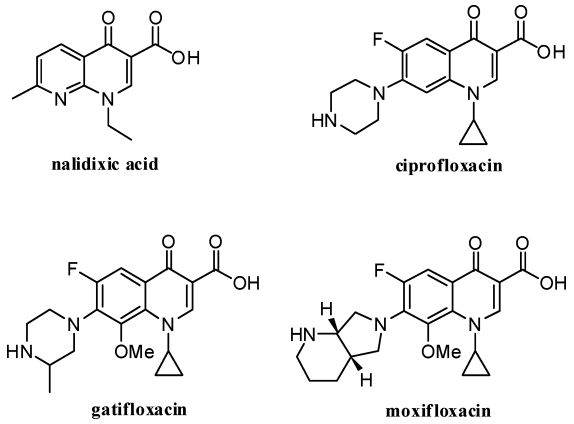

Figure 2. Structures of several 4-quinolones exhibiting antitrypanosomal activity.

The initial finding that the amidation of the carboxyl function resulted in antitrypanosomal activity in the low micromolar concentration range prompted us to synthesize and test a library of quinolone-type molecules mainly characterized by a benzylamide function in position 3 and an amine heterocycle in position 7. A subsequent SAR analysis indicated the importance of the amide group.

Screening to elucidate the target of these newly synthesized compounds in trypanosomes was performed using a range of organelle marker cell lines and fluorescence microscopy. Initially observed changes in mitochondrion morphology were followed up by a cell cycle analysis, which revealed that kinetoplast segregation was affected. Because compound **29** exhibited promising in vitro activity against *T. b. brucei* and *T. b. rhodesiense*, it was also tested in vivo in the *T. b. rhodesiense* (STIB900) acute mouse model.

RESULTS AND DISCUSSION

Chemistry. The syntheses of 4-oxo-quinoline skeletons were accomplished according to the Gould−Jacobs procedure, starting off with the condensation of 3-chloro-4-fluoroaniline **1a** and 3-(trifluoromethyl)-aniline **1b**, respectively, with diethyl 2-(ethoxymethylene)-malonate (EMME). Subsequent cyclization in boiling diphenyl ether resulted in ethyl 7-chloro-6-fluoro-4-hydroxyquinoline-3-carboxylate **3a** and ethyl 7-(trifluoromethyl)-4-hydroxyquinoline-3-carboxylate **3b**.[17−19] In both cases regioisomers arose, where ethyl 5-chloro-6-fluoro-4-hydroxyquinoline-3-carboxylate **3a′** and ethyl 5-(trifluoromethyl)-4-hydroxyquinoline-3-carboxylate **3b′** were obtained in low amounts (<5%). Hence these isomer mixtures were carried on to the next step without separation. The alkylation of position 1 was achieved with corresponding alkyl halides in the presence of potassium carbonate.[20] After separation of the regioisomers using normal phase column chromatography on silica gel and hydrolysis of the ethyl ester, the corresponding 4-oxo-1,4-dihydroquinoline-3-carboxylic acids **4a−c** were isolated in good yields.[19,20] 7-Chloro-1-cyclopropyl-6-fluoro-4-oxo-1,4-dihydroquinoline-3-carboxylic acid **4d** was commercially available. Ethyl 7-(trifluoromethyl)-4-oxo-1,4-dihydroquinoline-3-carboxylic acid **4b** was amidated in position 3 using *i*-

dx.doi.org/10.1021/jm101439s | J. Med. Chem. 2012, 55, 2538−2548

Scheme 1[a]

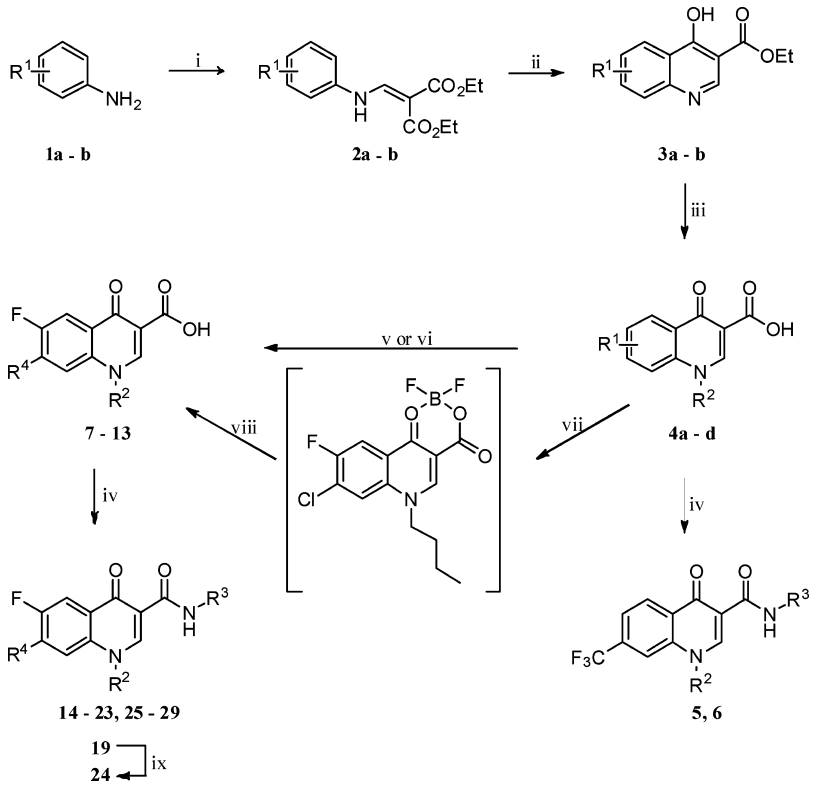

[a]Reagents and conditions: (i) EMME, toluene, reflux; (ii) diphenyl ether, reflux; (iii) (1) alkyl halide, K_2CO_3, KI, DMF, 80 °C, (2) KOH (2M), reflux; (iv) H_2NR^3, *i*-butyl chloroformiate, NMM, DMF_{abs}, 0 °C/rt; (v) piperidine/piperidine-4-carboxamide, DMF, 90 °C; (vi) morpholine/*N*-benzylmethylamine, MW (500 W), 120 °C; (vii) $BF_3{\cdot}OEt_2$, CH_2Cl_{2abs}, reflux; (viii) (1) DMF, 60 °C, (2) KOH (2M), reflux; (ix) BBr_3, CH_2Cl_{2abs}, 0 °C/rt.

butyl chloroformiate, *N*-methylmorpholine (NMM), and corresponding amines to give compounds **5** and **6**.[19] The 7-chloro-6-fluoro-4-oxo-1,4-dihydroquinoline-3-carboxylic acid derivatives **4a**, **4c**, and **4d** were used for the chloride substitution in position 7 with different cyclic and acyclic amines. The substitution of either **4a**, **4c**, or **4d** with piperidine or piperidine-4-carboxamide was carried out in DMF at 80 °C to give intermediates **7**–**10**.[19] This method did not work for compounds **11** and **12**. Hence, compounds **11** and **12** were obtained by dissolving **4c** in morpholine or *N*-benzylmethylamine and heating under microwave irradiation (120 °C/500 W/4 h). Compound **13** was prepared via the borate complex of **4c**.[21] The boron ester was accomplished using boron trifluoride diethyl etherate and served as internal Lewis acid, which activates position 7 for nucleophilic aromatic substitution. The chloride substitution was achieved in DMF containing a huge amount of free dimethyl amine. Subsequent hydrolysis led to intermediate **13**. For amidation in position 3, the carboxylic acids were activated using *i*-butyl chloroformiate and NMM. Subsequently, the in situ generated mixed anhydride was converted with different aryl amines to give the corresponding amides **14**–**23** and **25**–**29**. Demethylation of compound **19** with BBr_3 resulted in compound **24** (Scheme 1).

To introduce a phenyl residue in position 7, the Suzuki coupling reaction was employed. Often, the oxidative addition is the rate-determining step in the catalytic process and is improved using aryl-bromides instead of aryl-chlorides.[22] Therefore, the ethyl 7-bromo-4-quinolone-3-carboxylate intermediate **32** was synthesized starting off with 1-bromo-2-fluorobenzene (Table 1). Nitration and reduction with iron and methanol was accomplished according to Austin et al., yielding the aniline **30**.[23] Subsequent condensation with EMME and cyclization in boiling diphenyl ether resulted in ethyl 7-bromo-6-fluoro-4-hydroxyquinoline-3-carboxylate **31**, which was alkylated in position 1 with brombutane in the presence of potassium carbonate and purified using normal phase column chromatography.[20,24] The Suzuki reaction was performed with phenylboronic acid in the presence of $Pd(OAc)_2$ and triphenylphosphine under basic conditions.[25] After ester hydrolysis, the amidation of position 3 resulted in compound **34** (Scheme 2).

Structure–Activity Relationships. Since the antitrypanosomal activity of ciprofloxacin and corresponding derivatives was reported,[8,12–16] we synthesized a quinolone-type library and tested the intermediates of the synthetic pathway as well as the 4-quinolone-3-carboxamides against *Trypanosoma brucei*. The antitrypanosomal activity was evaluated in *Trypanosoma brucei brucei* according to Räz et al., and cytotoxicity was measured in macrophages J774.1 using the AlamarBlue-based assay.[26–28] These data are displayed in Table 2. The most active compound is the morpholino-substituted substance **29** having an IC_{50} (*T. b. brucei*) of 0.047 μM and an IC_{50} value of 0.009 μM against the human pathogenic subspecies *T. b. rhodesiense* (STIB900).

The intermediate 4-hydroxy-quinoline esters **3a**–**b** (data not shown) and 4-quinolone carboxylic acids **4a**–**d** did not show any activity. After amidation of **4b** in position 3, resulting in compound **5**, the IC_{50} value decreased to 7.31 μM. Comparing

dx.doi.org/10.1021/jm101439s | *J. Med. Chem.* 2012, 55, 2538–2548

Table 1. Substitution Pattern of Intermediates and 4-Quinolone-3-carboxamide Derivatives 4−34

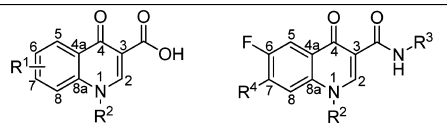

Compd.	R^1 / R^4	R^2	R^3	Compd.	R^1 / R^4	R^2	R^3
4a	Pos. 6 = F Pos. 7 = Cl	*n*-Pr	-	**16**		*n*-Bu	
4b	Pos. 7 = CF_3	Et	-	**17**			
4c	Pos. 6 = F Pos. 7 = Cl	*n*-Bu	-	**18**		*n*-Pr	
5	Pos. 7 = CF_3	Et	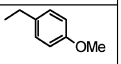	**19**		*n*-Bu	
6	Pos. 7 = CF_3	Et	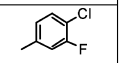	**20**			
7		*n*-Pr	-	**21**		*n*-Pr	
8		*n*-Bu	-	**22**		*n*-Bu	
9			-	**23**		*n*-Bu	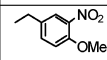
10		*n*-Bu	-	**24**	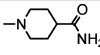	*n*-Bu	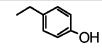
11		*n*-Bu	-	**25**	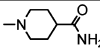	*n*-Bu	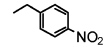
12		*n*-Bu	-	**26**		*n*-Bu	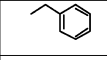
13		*n*-Bu	-	**27**		*n*-Bu	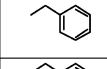
14			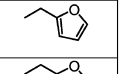	**28**		*n*-Bu	
15		*n*-Pr		**29**		*n*-Bu	
				34		*n*-Bu	

Scheme 2[a]

[a]Reagents and conditions: (i) (1) HNO_3, H_2SO_4, 0 °C/rt, (2) Fe, MeOH, reflux; (ii) (1) EMME, toluene, reflux, (2) diphenyl ether, reflux; (iii) brombutane, K_2CO_3, KI, DMF, 80 °C; (iv) (1) phenylboronic acid, $Pd(OAc)_2$, PPh_3, K_2CO_3, DMF/H_2O (9:1), 60 °C, (2) KOH (2M), reflux; (v) benzylamine, *i*-butyl chloroformiate, NMM, DMF_{abs}, 0 °C/rt.

benzylamides (**5**) with phenylamides (**6**) revealed the amidation in position 3 to be essential for high activity, but only for benzylamide and not for phenylamide derivatives, indicating the need of flexible aromatic moieties in position 3.

The replacement of the chloride atom with cyclic and acyclic amines in position 7, giving the 4-quinolone derivatives **7**−**13**, results in inactive or low activity. However, again the subsequent amidation of 4-quinolone-3-carboxylic acids **7**−**13**

dx.doi.org/10.1021/jm101439s | *J. Med. Chem.* 2012, 55, 2538−2548

Table 2. Antitrypanosomal Activity, Cytotoxicity, and Selectivity Index of 4-Quinolone-3-carboxamide Derivatives and Intermediates[a]

	T. brucei brucei IC_{50} [μM]			
compd	48 h (sdv)	72 h (sdv)	cytotoxicity J774.1 IC_{50} [μM]	selectivity index (SI)
4a	>40	>40	>100	>2.50
4b	>40	>40	>100	>2.50
4c	>40	>40	>100	>2.50
5	7.31 (2.29)	6.37 (1.25)	>100	>13.7
6	>40	>40	>100	>2.50
7	>40	>40	>100	>2.50
8	>40	>40	>100	>2.50
9	>40	>40	>100	>2.50
10	14.6 (0.51)	18.1 (0.6)	93.0	6.39
11	19.2 (2.36)	22.2 (2.82)	>100	>5.21
12	17.2 (1.00)	23.0 (8.15)	43.2	2.51
13	>40	>40	>100	>2.50
14	8.89 (4.17)	12.1 (2.15)	>100	>11.2
15	4.60 (0.53)	4.84 (0.76)	56.9	12.4
16	1.03 (0.13)	1.84 (0.32)	41.4	40.2
17	2.75 (0.31)	2.56 (1.12)	>100	>36.4
18	2.28 (0.51)	3.12 (1.19)	41.4	18.2
19	0.78 (0.14)	1.45 (0.61)	40.8	52.3
20	1.07 (0.16)	1.91 (0.65)	51.2	47.9
21	0.75 (0.23)	1.25 (0.20)	43.7	58.3
22	1.09 (0.47)	1.98 (0.80)	47.0	43.1
23	3.07 (0.59)	4.14 (0.48)	>100	>32.6
24	3.09 (0.56)	5.12 (0.14)	41.6	13.5
25	0.54 (0.14)	0.58 (0.14)	>100	>185.2
26	0.67 (0.11)	1.04 (0.22)	47.8	71.3
27	5.40 (0.55)	10.77 (1.37)	86.0	15.9
28	0.68 (0.16)	0.92 (0.01)	>100	>147.1
29	0.047 (0.00)	0.05 (0.01)	57.0	1140
	0.009[b]			6333[b]
34	>40	>40	>100	>2.50

[a]All compounds are tested in duplicate to calculate mean value and standard deviation (sdv). For comparison: pentamidine diisethionate IC_{50} = 0.0029 μM; suramine Na IC_{50} = 0.31 μM; eflornitine HCl IC_{50} = 22.9 μM; melarsoprol IC_{50} = 0.0026 μM. [b]Activity of compound **29** against *T. b. rhodesiense* and corresponding selectivity index.

exhibited an enhancement in activity. This finding clearly demonstrated that a combination of benzylamides in position 3 and cyclic and acyclic amines in position 7 are necessary for high antitrypanosomal activity. In the following, structure–activity relationships of 7-amino-substituted 4-quinolone-3-carboxamides will be discussed in detail:

1. The Influence of Alkyl Substituents in Position ***1****.* Comparison of derivatives **14**–**16**, **17**–**19**, and **20**–**22** with either cyclopropyl-, *n*-propyl-, or *n*-butyl-residues in position 1 revealed *n*-butyl-substituted 4-quinolones of compounds **13**–**15** and **16**–**18** to be advantageous, e.g., *N*-butyl compound **19** exhibited an IC_{50} value of 0.78 μM while the *N*-cyclopropyl compound **17** showed an IC_{50} value of 2.75 μM. However, the comparison of compounds **20**–**22** revealed the *n*-propyl-substituted compound **21** to have the lowest IC_{50} value. Nevertheless, the longer alkyl chains in position 1 the higher is the activity.

2. Carboxylic Acid versus Aromatic Amide Function in Position ***3****.* Comparison of the acid derivatives with the amide compounds revealed the benzylamide residue in position 3 to be pivotal. This finding is supported by the fact that most fluoroquinolone acid derivatives reported in the literature were found to exhibit at most a weak activity.[12−16] Moreover, no in vivo effectivity was found for these acids in mice.[15]

3. The Influence of the Phenyl Substitution of the Benzylamides in Position ***3****.* The comparison of the benzylamide, compounds **19** and **22**–**25** exhibited, that either a nitro or methoxy group induces a high activity in comparison to a hydroxy group (**24**) and a combination of methoxy and nitro group (**23**). This result indicated that nitro and methoxy groups, which can be regarded as H-bond acceptors, led to higher trypanocidal activities than H-bond donors like the hydroxy group. An additional H-bond acceptor on the aromatic moiety decreased the activity (**23**). This might be due to steric hindrance.

4. The Influence of Cyclic and Acyclic Amines in Position ***7****.* To examine the influence of different amines, we have chosen the *n*-butyl substituent in position 1 and the benzylamide in position 3 and varied the amine substituent in position 7. Whereas compounds **22** and **27** carrying a *N*-benzylmethylamine and a piperidine-4-carboxamide, respectively, showed low activity, the piperidino- and *N*,*N*-dimethylamino substituted compounds **26** and **28**, respectively, are active in the submicromolar range of concentration. They were even surpassed by the morpholino-substituted derivative **29** showing an IC_{50} value of 47 nM. Because smaller substituents like piperidine, morpholine, and *N*,*N*-dimethylamine showed higher activity, steric hindrance might play a pivotal role. Morpholine comprises a H-bond acceptor, which might enable interactions at this position.

By means of the Suzuki reaction, a phenyl residue could be realized in position 7. The resulting compound **34** showed an IC_{50} value above 40 μM and emphasizes the need of saturated N–C coupled substituents in this position.

Physicochemical Properties and Formulation. The pK_a of lead compound **29** was determined UV metrically at 4.53 ± 0.18 (n = 6) and corroborated potentiometrically (pK_a of 4.63). The lipophilicity of the most active compounds **16**, **19**, **20**, **21**, **22**, **25**, **26**, **28**, and **29** was determined using RP HPLC and the correlation between the capacity factor k' and the logP values of reference compounds.[29] The logP values range from 2.4 to 4.0, and the molecular weight of the most active compounds is in the range of 395.5 g/mol and 523.6 g/mol. Additionally, all compounds comprise less than 10 H-bond acceptors and less than 5 H-bond donors, respectively. These properties correlate with Lipinski's Rule of Five and predict a good oral bioavailability.[30]

The solubility of compound **29** in buffered aqueous media has been assessed in preliminary tests, ranking the compound as "poorly water-soluble" or slightly soluble or less according to USP or EP pharmacopeial terminology. Drug solubility in water is typically a function of (i) entropy of mixing, (ii) drug–drug interactions associated with lattice energy in cases the drug is crystalline, and (iii) the difference of adhesive interactions (drug–water) and the sum of cohesive interactions (water–water and drug–drug). The crystal structure of **26** (Figure 3), one representative of this group of compounds, indicates such high crystal forces. Compound **29** has a sharp melting point determined at 164–165 °C (n = 3), further supporting the assumption of rather strong crystal forces and arguably pointing to the development of a formulation, within which compound **29** is presented in amorphous form or dissolved state.

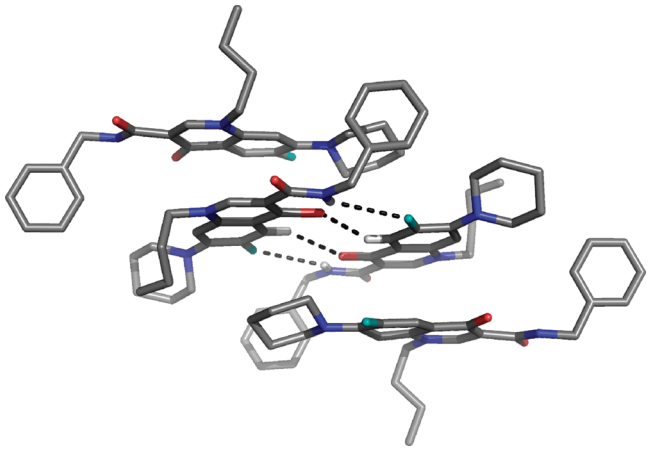

Figure 3. Distinctive layers of compound **26**. Two molecules in a plane communicate via weak intermolecular H-bond interaction of the aromatic proton at C5 and the carbonyl oxygen in position 4 (about 2.2−2.6 Å) as well as the fluoride atom at C6 and the amide proton (about 3.1 Å). The distance between the aromatic skeleton of two molecules is about 3.6 Å, indicating a possible interaction of π-electronic systems.

For in vivo experiments, common aqueous DMSO mixtures for dissolving **29** could not be used. Even the addition of 10% of typical used surface-formulation ingredients like Tween 80 or Cremophor RH40 did not substantially improve the water solubility of compound **29**. Thus, a preliminary oral formulation consisting of Cremophor RH40 (35%), Capmul MCM C8 (45%), triethylcitrate (10%), and ethanol (10%) was developed which dissolves a concentration of 10 mg/mL of **29** and forms stable emulsions in aqueous solutions (stable >24 h). The developed preconcentrate is suitable for oral use, and similar formulations have been deployed.[31] However, responses to parenteral administration require further characterization, particularly hemodynamic response in vitro and in vivo responses (acid−base balance, blood gases, plasma electrolytes, and arterial blood pressure or heart rate) due to ascending doses of the vehicle should be characterized prior to using the formulation.[32]

In Vivo Activity and Target Search. An aqueous 1:1 dilution of the formulation, containing 10 mg/mL of **29**, was administered orally to *T. b. rhodesiense* (STIB900) infected NMRI mice. Compound **29** did not show in vivo efficacy at an oral dose of 50 mg/kg given on four consecutive days. In the absence of pharmacokinetic data, we cannot distinguish if this is due to missing in vivo efficacy or related to the bioavailability of the compound when delivered in strongly solubilized form, as done in this study. Future studies will detail the interaction of the compound with the different elements constituting the micelles in the administered microemulsion, and appropriate dissolution and pharmacokinetic studies should detail this aspect. Strong solubilization has been demonstrated to constitute an important parameter affecting the drug bioavailability and, hence, bioactivity.[33] As discussed before, the formulation is not yet suitable for parenteral use.

The target of the quinolone-3-carboxylic acids was shown to be the topoisomerase II of the trypanosome.[8,14,15] However, because the carboxylate function is essential for the interaction of the drugs with the topoisomerase, it is quite likely that the benzylamides address a different target.

To narrow down the target of these antitrypanosomal compounds, **19** and **29** were subjected to a fluorescence microscopy based screen. Recombinant marker cell lines, in which organelles are fluorescently labeled by GFP or YFP fusion to an organelle specific resident protein, were employed to study the effect of the two compounds on the mitochondrion, Golgi, ER, endosomes, and lysosome of the cell. No significant changes in the morphology of the Golgi, ER, endosomes, or lysosome could be observed. However, incubation with both compounds **19** (0.54 ± 0.04 μM) and **29** (0.023 ± 0.004 μM) at IC_{50} concentrations for 42 h suggested a change in the morphology of the mitochondrion compared to control cells. In untreated BSF *T. brucei*, the mitochondrion is an elongated, tubular structure extending the length of the cell. In cells treated with both compound **19** and **29**, mitochondrion morphology appeared altered, showing sheet-like patches in the cell-spanning mitochondrion. Figure 4 shows the observed phenotype with representative cells.

As it is known that ciprofloxacin acts as a topoisomerase II inhibitor and compounds **19** and **29** are quinolone-type structures, we further focused on the kinetoplast. A cell cycle analysis of chemical treated cells showed that compounds **19** and more so **29** revealed an increased percentage of 1K1N cells displaying segregating kinetoplasts, $1K^{seg}1N$, suggesting that both compounds interfere with correct segregation of the kinetoplast (Figure 5). The insert in Figure 5 shows a cell displaying a stark segregation defect. This phenotype was not evident in ciprofloxacin treated cells. To further investigate the

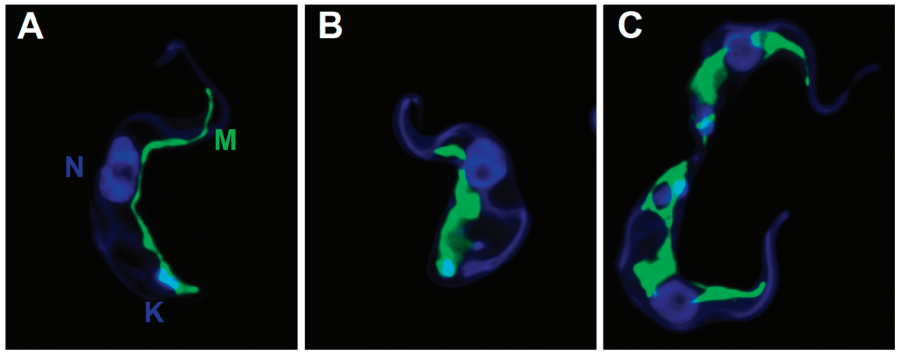

Figure 4. Fluorescence microscopy images of a *T. b. brucei* mitochondrion marker cell line treated with DMSO (A), compound **19** (B), and compound **29** (C). The mitochondrion, M, is shown in green. The cell surface (AMCA stained) and the nucleus, N, and kinetoplast, K, (DAPI stained) are shown in blue. Whereas control cells (A) show the typical elongated, tubular structure of the mitochondrion of BSF trypanosomes, cells treated with compounds **19** or **29** (B, C) show sheet-like patches in the tubular structure.

dx.doi.org/10.1021/jm101439s | *J. Med. Chem.* 2012, 55, 2538−2548

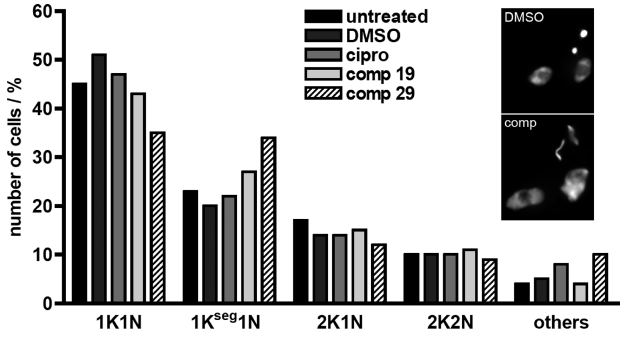

Figure 5. Cell cycle analysis of a *T. b. brucei* mitochondrion marker cell line before and after treatment for 42 h with DMSO, ciprofloxacin, compound **19**, and compound **29** (n = 300 each). Treatment with compounds **19** and **29** lead to a shift in ratio of 1K1N to $1K^{seg}1N$ cells from 2:1 to 3:2 and 1:1, respectively. The inset shows cells that have been stained with DAPI to show the larger nucleus and smaller kinetoplast. The upper figure (DMSO) shows two typical cells, whereas the lower figure (comp) depicts a stark example of two cells displaying a segregation defect in their kinetoplasts.

possibility that compounds **19** and **29** target the mitochondrial topoisomerase II, $TbTopoII_{mt}$, of *T. brucei*, we knocked down $TbTopoII_{mt}$ in BSF cells by RNA interference. The function of this $TbTopoII_{mt}$ in trypanosomes has been studied previously in insect stage trypanosomes employing RNA interference.[34,35] These studies showed that knockdown of $TbTopoII_{mt}$ lead to a shrinkage and eventual loss of the kinetoplast. Knockdown of $TbTopoII_{mt}$ in BSF trypanosomes produced a comparable phenotype, where the kinetoplast was lost over time (Figure 6). However, a segregation defect could not be detected, not even transiently. This formally excludes the possibility that compounds **19** and **29** target $TbTopoII_{mt}$ alone but suggests these compounds also affect other proteins involved in *T. brucei* kinetoplast segregation. This is in line with previous findings that only β-keto-carboxylates are able to closely bind to the topoisomerase II[36] which, in turn, the amides cannot, indicating that the topoisomerase is likely not the target of the quinolone-amides.

CONCLUSION

The biological evaluation of the 4-quinolone-3-carboxamide library revealed several promising lead compounds with antitrypanosomal activity in the nanomolar concentration range and low cytotoxicity. The SAR analysis illustrated the need of alkyl chains in position 1, benzylamides in position 3, and amine heterocycles in position 7 and led to compound **29** with an IC_{50} (*T. b. brucei*) of 47 nM and an IC_{50} value against *T. b. rhodesiense* of 9 nM. Moreover, because the most active compounds show a cytotoxicity higher than 40 μM, the gap between trypanocidal activity and cytotoxicity augments with increasing antiinfective activity, resulting in an SI value of 6333 for compound **29**. Furthermore, the main advantage of this group of compounds is the simple route of synthesis using the well-known Gould–Jacobs procedure, which gives good overall yields.

For identifying the target of these compounds, the antitrypanosomal substances **19** and **29** were subjected to a fluorescence microscopy based screen. Incubation with both compounds appeared to affect the morphology of the mitochondrion. Further analysis revealed that trypanosomes

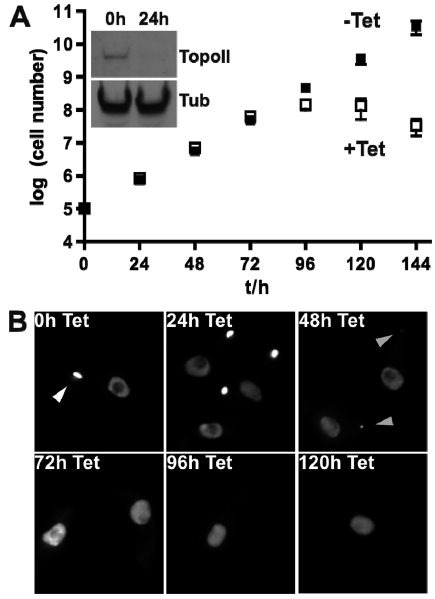

Figure 6. Knockdown of mitochondrial *T. brucei* topoisomerase II. (A) Knockdown of $TbTopoII_{mt}$ in BSF trypanosomes affects cell growth beginning 72 h after induction of RNAi with tetracycline (Tet). Three independent clones were analyzed, and cell numbers in the growth curves are shown as the average of these and their standard deviation. The inset shows a Northern blot analysis of one clone to confirm knockdown of topoisomerase II (TopoII) mRNA 24 h after induction of RNAi. Tubulin (Tub) mRNA served as a loading control. (B) Images illustrating the shrinkage of the kinetoplast over time after RNAi induction. At 0 h, kinetoplasts are clearly visible (indicated by a white arrowhead). kDNA loss of DAPI stained cells is first detected after 48 h of induction (indicated by gray arrowheads). By 72 h post induction, the majority of cells are dyskinetoplastid.

treated with these compounds showed a defect in kinetoplast segregation.

Compound **29** was selected for evaluation in a murine model of human African trypanosomiasis. Therefore, a preliminary formulation was developed, but oral administration proofed ineffective against *T. b. rhodesiense* (STIB900) infected NMRI mice. Nevertheless, the outstanding in vitro activity of **29** aganist *T. b. brucei* and *T. b. rhodesiense* suggests that this compound serves as a promising lead structure for further optimization. Thus, structural modification of **29** for increasing the water solubility, as well as developing a more appropriate parenteral formulation, will be the future goal.

EXPERIMENTAL SECTION

Melting points were determined with a Stuart melting point apparatus SMP11 (Bibby Scientific, UK) and not corrected. IR spectra were obtained using a Biorad PharmalyzIR FT-IR spectrometer (Digilab, Krefeld, Germany). TLC was performed on silica gel 60 F_{254} aluminum sheets (Merck, Darmstadt, Germany). ^1H (400.132 MHz) and ^{13}C (100.613 MHz) NMR spectra were recorded on a Bruker AV 400 instrument (Bruker Biospin, Ettlingen, Germany). As internal standard, the signals of the deuterated solvents were used (DMSO-d_6: ^1H 2.5 ppm, ^{13}C 39.52 ppm; $CDCl_3$: ^1H 7.26 ppm, ^{13}C 77.16 ppm). Abbrevations for data quoted are: s, singlet; d, doublet; t, triplet; q, quartet; m, multiplet; b, broad; dd, doublet of doublets; dt, doublet of triplets; tt, triplet of triplets; tq, triplet of quartets. Coupling constants (J) are given in Hz. Chemicals were of analytical grade and purchased from Aldrich (Steinheim, Germany) and Merck (Darmstadt, Germany).

dx.doi.org/10.1021/jm101439s | J. Med. Chem. 2012, 55, 2538–2548

The purities of new compounds was determined using microanalysis (C, H, N) and HPLC and agreed with the theoretical value within ±0.4% and ≥95%, respectively. Alternatively, HPLC analyses were performed on an Agilent 1100 HPLC system with UV detector, using a C18 reversed-phase Inertsil ODS-2 column (150 × 4.6 mL, 5 μm) eluting with a mixture of methanol/phosphate buffer (Method 1, 70% methanol:30% phosphate buffer. Method 2: gradient, 30% methanol going up to 80% methanol in 5 min, 80% methanol going down to 30% methanol in 5 min, 30% methanol for 2 min. Flow rate 1.0 mL/min, λ = 254.4 nm.).

Syntheses of compounds **3a**, **3b**, **4a**, **4b**, **5**, **6**, **9**, **30**, and **31** were performed according to refs 18−20, 23, and 24.

Synthesis of 1-Butyl-7-chloro-6-fluoro-4-oxo-1,4-dihydroquinoline-3-carboxylic Acid (4c). **3a** (1 equiv) and potassium carbonate (5 equiv) were suspended in DMF (15 mL) at rt. After 15 min of stirring, a catalytic amount of potassium iodide and 6 equiv of 1-bromobutane were added and the mixture was stirred at 80 °C for 24 h. After cooling to rt, the solvent was removed in vacuo and the residue was purified by column chromatography on silica gel (eluent: $CHCl_3$/MeOH = 15:1, R_f = 0.66). The resulting ethyl 1-butyl-7-chloro-6-fluoro-4-oxo-1,4-dihydroquinoline-3-carboxylate was suspended in 20 mL of aqueous sodium hydroxide solution (2M) and refluxed for 4 h. After cooling to rt, the solution was acidified by means of concentrated hydrochloride acid (pH = 4). The precipitate was collected, washed with a mixture of water and acetone (1:1), and dried in vacuo to give compounds **4c**.

Yield 87%; mp 233−236 °C. IR [cm^{-1}]: 3048, 2959, 2872, 1717, 1610, 1458, 1032, 897, 808. ^{1}H NMR (DMSO-d_6, δ [ppm], J [Hz]): 14.7 (s, 1H), 9.03 (s, 1H), 8.40 (d, $^4J_{H,F}$ = 5.3, 1H), 8.13 (d, $^3J_{H,F}$ = 8.6, 1H), 4.56 (t, ^3J = 7.0, 2H), 1.74 (tt, ^3J = 7.0, ^3J = 7.0, 2H), 1.34 (tq, ^3J = 7.0, ^3J = 7.0, 2H), 0.90 (t, ^3J = 7.0, 3H). ^{13}C NMR (DMSO-d_6, δ [ppm], J [Hz]): 176.5 (d, $^4J_{C,F}$ = 2.2), 165.5, 154.9 (d, $^1J_{C,F}$ = 249.6), 150.0, 136.4 (d, $^4J_{C,F}$ = 2.2), 127.4 (d, $^2J_{C,F}$ = 20.5), 123.3 (d, $^3J_{C,F}$ = 6.5), 121.1, 111.9 (d, $^2J_{C,F}$ = 22.7), 107.7, 53.8, 30.8, 19.0, 13.5. Anal. ($C_{14}H_{13}ClFNO_3$) Calcd: C 56.5, H 4.40, N 4.70. Found: C 56.3, H 4.67, N 4.48.

Synthesis of 1-Butyl-7-(4-carbamoylpiperidin-1-yl)-6-fluoro-4-oxo-1,4-dihydroquinoline-3-carboxylic Acid (8). **4c** (1 equiv) and piperidine-4-carboxamide (8 equiv) were dissolved in DMF (20 mL) and stirred at 80 °C for 24 h. The solvent was removed in vacuo and the residue resuspended in water (20 mL). After acidification with concentrated hydrochloride acid (pH = 4), the mixture was stirred for 15 min at rt. The solid was filtered, washed several times with water, and dried in vacuo to give compound **8**.

Yield 52%; mp 226−228 °C. IR [cm^{-1}]: 3196, 3049, 2951, 2872, 1716, 1625, 1472, 936, 808. ^{1}H NMR (DMSO-d_6, δ [ppm], J [Hz]): 15.3 (s, 1H), 8.90 (s, 1H), 7.85 (d, $^3J_{H,F}$ = 13.1, 1H), 7.32 (s, 1H), 7.12 (d, $^4J_{H,F}$ = 6.0, 1H), 6.83 (s, 1H), 4.54 (t, ^3J = 7.0, 2H), 3.72−3.70 (m, 2H), 2.97−2.92 (m, 2H), 2.35−2.33 (m, 1H), 1.85−1.76 (m, 6H), 1.33 (tq, ^3J = 7.0, ^3J = 7.0, 2H), 0.92 (t, ^3J = 7.0, 3H). ^{13}C NMR (DMSO-d_6, δ [ppm], J [Hz]): 176.0 (d, $^4J_{C,F}$ = 2.0), 175.8, 166.1, 152.9 (d, $^1J_{C,F}$ = 249.5), 148.7, 145.7 (d, $^2J_{C,F}$ = 10.3), 137.5, 118.9 (d, $^3J_{C,F}$ = 6.6), 111.0 (d, $^2J_{C,F}$ = 23.7), 106.8, 105.8 (d, $^3J_{C,F}$ = 3.7), 53.3, 49.4 (2C), 40.9, 30.3, 28.2 (2C), 19.1, 13.4. HPLC purity (method 2): 94.64%.

Synthesis of 1-Butyl-6-fluoro-7-morpholino-4-oxo-1,4-dihydroquinoline-3-carboxylic Acid (11). **4c** (1 equiv) was dissolved in morpholine (10 mL) and heated under microwave irradiation (500W/120 °C) for 4 h. After cooling to rt, 20 mL of water were added and the solution was acidified with concentrated hydrochloride acid (pH = 4). The precipitated solid was filtered and washed with water to give compound **11** after drying in vacuo.

Yield 68%; mp 242−243 °C. IR [cm^{-1}]: 3019, 2968, 2172, 1720, 1626, 1460, 1257, 942, 804. ^{1}H NMR ($CDCl_3$, δ [ppm], J [Hz]): 14.8 (s, 1H), 8.61 (s, 1H), 8.04 (d, $^3J_{H,F}$ = 13.1, 1H), 6.86 (d, $^4J_{H,F}$ = 6.8, 1H), 4.22 (t, ^3J = 7.1, 2H), 3.92−3.90 (m, 4H), 3.29−3.27 (m, 4H), 1.88 (tt, ^3J = 7.1, ^3J = 7.5, 2H), 1.43 (tq, ^3J = 7.5, ^3J = 7.2, 2H), 0.99 (t, ^3J = 7.2, 3H). ^{13}C NMR ($CDCl_3$, δ [ppm], J [Hz]): 176.7 (d, $^4J_{C,F}$ = 2.5), 166.8, 153.2 (d, $^1J_{C,F}$ = 252.2), 147.5, 145.3 (d, $^2J_{C,F}$ = 9.9), 136.9, 120.8 (d, $^3J_{C,F}$ = 8.7), 112.7 (d, $^2J_{C,F}$ = 23.0), 108.0, 103.7 (d, $^3J_{C,F}$ = 3.3), 66.6 (2C), 51.4, 49.9 (2C), 30.5, 19.6, 13.3. Anal. ($C_{18}H_{21}FN_2O_4$) Calcd: C 62.1, H 6.08, N 8.04. Found: C 62.0, H 6.24, N 7.80.

General Procedure for the Syntheses of 1-Butyl-7-(4-carbamoylpiperidin-1-yl)-6-fluoro-*N*-(4-methoxybenzyl)-4-oxo-1,4-dihydroquinoline-3-carboxamide (19) and *N*-Benzyl-1-butyl-6-fluoro-7-morpholino-4-oxo-1,4-dihydroquinoline-3-carboxamide (29). 4-Oxo-quinolone-3-carboxylic acid (1 equiv) and NMM (5 equiv) were dissolved in abs DMF (10 mL) at rt under Ar atmosphere. After cooling to 0 °C, 4 equiv of *i*-butyl chloroformiate were added and the mixture was stirred for 1 h. Then 4 equiv of the corresponding amine were added and the mixture was stirred for additional 2 h at rt. The solvent was removed in vacuo, and 20 mL of water were added. The aqueous solution was extracted three times with ethyl acetate (150 mL). The combined organic layers were dried over sodium sulfate. The solvent was reduced in vacuo, and the residue was purified by normal phase column chromatography on silica gel.

1-Butyl-7-(4-carbamoylpiperidin-1-yl)-6-fluoro-*N*-(4-methoxybenzyl)-4-oxo-1,4-dihydroquinoline-3-carboxamide (19). Yield 46%; mp 195−196 °C. eluent: $CHCl_3$/MeOH = 20:1 (R_f = 0.43). IR [cm^{-1}]: 3193, 2931, 2868, 2833, 1653, 1488, 1233, 1031, 803. ^{1}H NMR (DMSO-d_6, δ [ppm], J [Hz]): 10.3 (t, ^3J = 5.7, 1H), 8.76 (s, 1H), 7.83 (d, $^3J_{H,F}$ = 13.4, 1H), 7.31 (s, 1H), 7.27 (d, ^3J = 8.6, 2H), 7.07 (d, $^4J_{H,F}$ = 7.1, 1H), 6.90 (d, ^3J = 8.6, 2H), 6.82 (s, 1H), 4.47−4.46 (m, 4H), 3.73 (s, 3H), 3.67−3.64 (m, 2H), 2.91−2.85 (m, 2H), 2.35−2.29 (m, 1H), 1.87−1.69 (m, 6H), 1.32 (tq, ^3J = 7.2, ^3J = 7.3, 2H), 0.92 (t, ^3J = 7.3, 3H). ^{13}C NMR (DMSO-d_6, δ [ppm], J [Hz]): 176.0, 174.1 (d, $^4J_{C,F}$ = 2.2), 164.0, 158.3, 152.6 (d, $^1J_{C,F}$ = 248.1), 147.7, 144.9 (d, $^2J_{C,F}$ = 11.0), 136.7, 131.5, 128.8 (2C), 121.2 (d, $^3J_{C,F}$ = 6.6), 113.8 (2C), 111.3 (d, $^2J_{C,F}$ = 22.7), 110.0, 105.7 (d, $^3J_{C,F}$ = 2.2), 55.1, 52.8, 49.5 (2C), 41.6, 41.0, 30.3, 28.3 (2C), 19.2, 13.5. HPLC purity (method 1): 98.29%.

***N*-Benzyl-1-butyl-6-fluoro-7-morpholino-4-oxo-1,4-dihydroquinoline-3-carboxamide (29).** Yield 58%; mp 164−165 °C. Eluent: ethyl acetate (R_f = 0.57). IR [cm^{-1}]: 3039, 2957, 2855, 1650, 1488, 1258, 1117, 929, 732. ^{1}H NMR (DMSO-d_6, δ [ppm], J [Hz]): 10.4 (t, ^3J = 5.9, 1H), 8.79 (s, 1H), 7.86 (d, $^3J_{H,F}$ = 13.6, 1H), 7.35−7.24 (m, 5H), 7.08 (d, $^4J_{H,F}$ = 7.3, 1H), 4.55 (d, ^3J = 5.9, 2H), 4.47 (t, ^3J = 7.1, 2H), 3.80−3.78 (m, 4H), 3.26−2.23 (m, 4H), 1.76 (tt, ^3J = 7.1, ^3J = 7.0, 2H), 1.33 (tq, ^3J = 7.0, ^3J = 7.4, 2H), 0.92 (t, ^3J = 7.4, 3H). ^{13}C NMR (DMSO-d_6, δ [ppm], J [Hz]): 174.0 (d, $^4J_{C,F}$ = 2.2), 164.1, 152.4 (d, $^1J_{C,F}$ = 247.1), 147.7, 144.3 (d, $^2J_{C,F}$ = 10.6), 139.3, 136.5, 128.3 (2C), 127.3 (2C), 126.8, 121.4 (d, $^3J_{C,F}$ = 6.8), 111.4 (d, $^2J_{C,F}$ = 22.7), 110.0, 105.5 (d, $^3J_{C,F}$ = 2.8), 65.8 (2C), 52.8, 49.8 (2C), 42.0, 30.2, 19.1, 13.4. Anal. ($C_{25}H_{28}FN_3O_3$) Calcd: C 68.6, H 6.45, N 9.60. Found: C 68.7, H 6.85, N 9.36.

Trypanosome Assay According to References 26 and 27. *Parasite Culture.* Trypomastigote forms of *T. brucei brucei* laboratory strain TC 221 were cultured in Baltz medium according to standard conditions.

In Vitro Cytotoxicity Assays. The test compounds were dissolved in DMSO or NaOH (0.1 M). A defined number of parasites (10^4 trypanosomes per mL) were exposed in test chambers of 96-well plates to various concentrations of the test substances in a final volume of 200 μL. Positive (trypanosomes in culture medium) and negative controls (test substance without trypanosomes) were run with each plate. The plates were then incubated at 37 °C in an atmosphere of 5% CO_2 for a total time period of 72 h. A reading was done at 48 h. The effect of test substances was quantified in IC_{50} values by linear interpolation of two different measurements. The activity of the test substances was measured by light absorption in an MR 700 microplate reader at a wavelength of 550 nm with a reference wavelength of 630 nm, using the AlamarBlue.

Macrophage Assay According to Reference 28. The macrophage cell line J774.1 was maintained in complete Click RPMI medium. For the experimental procedures, cells were detached from the flasks with a rubber police, washed twice with PBS, and suspended at 2 × 10^6 cells per mL in complete Click RPMI medium. J774.1 macrophages were plated in complete RPMI medium (200 μL) without phenol red in 96-well plates in the absence or presence of

dx.doi.org/10.1021/jm101439s | J. Med. Chem. 2012, 55, 2538−2548

various concentrations of the compounds and incubated for 24 h at 37 °C, 5% CO_2, 95% humidity. Following the addition of AlamarBlue (20 μL), the plates were further incubated at similar conditions. The plates were then read 24 and 48 h later. Control experiments to examine the effect of cell density, incubation time, and DMSO concentration were performed. Absorbance in the absence of compounds was set as 100% of growth control.

LogP Determination According to Reference 29 and pK_a Determination. *LogP Determination by Means of RP HPLC.* The partition coefficients of all compounds were determined by RP-chromatography using methanol/phosphate buffer 70:30 as an eluent. The chromatographic systems were calibrated with solutes for which an experimental octanol/water partition coefficient was available.[37] The capacity factors of the reference substances were correlated against with experimental octanol/water logP values, and the obtained correlation equation was used to calculate logP values of the tested compounds.

Liquid chromatography was conducted on an Agilent 1100 series system with a C18 reversed-phase Inertsil ODS-2 (MZ-Analytical, Mainz, Germany) (150 × 4.6 mL, 5 μm) column. The methanol (LiChrosolv, Merck, Germany)/buffer (70/30) mobile phase was used at a flow rate of 1.5 mL/min. The phosphate buffer (10 mM) was prepared by dissolving 1.361 g of potassium dihydrogen phosphate in Millipore water and adjusting the solution to pH 7.4 with aqueous sodium hydroxide solution (0.1 M). Then 0.02% *N*,*N*-dimethylhexylamine was added to minimize the peak tailing. The following aromatic compounds were applied for calibration: 2-phenylethanol, benzene, chlorobenzene, toluene, ethylbenzene, cumene, biphenyl, and anthracene.

First, 4 mg of the analytes were dissolved in 1 mL of DMSO (ACS spectrophotometric grade, Sigma-Aldrich, Germany). Then 10 μL of the DMSO solution were diluted with 990 μL of the mobile phase to a concentration of 4 μg/mL. Experiments were run in duplicate, and peak maxima were determined at 254.4 nm. Capacity ratios were determined as $k' = (t_r - t_o)/t_o$, where t_r is the average retention time of the analyte and t_o is the average retention time of the solvent. A linear regression was performed for the logk'/logP data of the reference compounds ($y = 2.3417x + 1.8415$; $r^2 = 0.9803$), and the regression equation was used to calculate the logP of the compounds.

pK_a was determined by UV assay using a Sirius T3 (Sirus; Forest Row, UK). The UV-based approach is particularly suitable for poorly water-soluble compounds with chromophores within five bond lengths of the ionizable group. For the experiment, 3 μL of a 10 mM stock of compound was used for each experiment ($n = 6$) and diluted with 1.5 mL of 0.15 KCl solution as starting solution and as described before.[38−40] This starting solution was titrated to pH 3 using 0.5 M HCl and titrated through a pH range of 3−9 using 0.5 M KOH. Absorbance was read over $\lambda = 200-700$ nm. The UV metric data was confirmed potentiometrically and as described before.[40] In brief, about 0.54 mg of compound was dissolved in 1150 μL of DMF. This solution was filled to 1.5 mL using 0.15 M KCl. The solution was titrated to pH 2 using 0.5 M HCl and titrated over a pH range of 2−12 thereafter and using 0.5 M KOH. Potentiometric changes were recorded by a pH electrode. Addition of DMF was required for the potentiometric approach due to solubility restrictions of compound **29**.

Microscopy and Image Analysis. *IC_{50} Determination.* IC_{50} values for ciprofloxacin and compounds **19** and **29** in the mitochondrion marker cell line were determined for 42 h of incubation. Each culture was set up in triplicate, and IC_{50} values were determined as described above with the exception of cell densities being determined by counting with a hemocytometer.

Sample Preparation. Organelle marker cell lines for the mitochondrion, Golgi, ER, endosomes, and lysosome were based on bloodstream form *T. b. brucei* 13.90 and cultured in HMI-9 at 37 °C and 5% CO_2. Following incubation with the respective chemical, dissolved in DMSO, for 42 h at IC_{50} concentrations or with 1% DMSO as a control, 5×10^6 to 1×10^7 cells were harvested at 1400*g* and 4 °C for 10 min. Cells were either washed twice in trypanosome dilution buffer (TDB; 5 mM KCl, 80 mM NaCl, 1 mM $MgSO_4$, 20 mM Na_2HPO_4, 2 mM NaH_2PO_4, 20 mM glucose, pH 7.4) and chemically fixed overnight in 2% formaldehyde at 4 °C or cell surface stained prior to fixing. For staining, cells were washed 3× with TDB and adjusted to a cell density of approximately 1×10^8 cells per mL. Cell surface labeling was performed by incubation with 1 mM sulfo-NHS-AMCA for 15 min on ice. After washing twice with TDB, cells were chemically fixed as described above. Before data acquisition, the nucleus and kinetoplast were stained by addition of DAPI.

Data Acquisition and Analysis. Image acquisition was performed with a Till Photonics iMic Microscope and the LA Live Acquisition software package. Three-dimensional images were acquired with 100× magnification and 150 nm × 100 nm *z*-step size. The acquired raw data was imported into the Huygens Essential Software (version 3.4, Scientific Volume Imaging, BV, Hilversum, The Netherlands) for digital deconvolution using the maximum likelihood algorithm and 100 iterations. Images of cells shown in Figures 4−6 were prepared by maximum intensity *z*-projection of the deconvolved stacks using ImageJ 1.42q (National Institutes of Health, USA).[41]

Knockdown of the Mitochondrial Topoisomerase II. A 500 bp fragment of the topoisomerase II gene[42] was amplified by PCR from Lister 427 genomic DNA. This fragment was cloned into a p2T7−177 RNAi expression vector[43] containing a puromycin cassette for selection.

First, 3×10^7 cells of the mitochondrion marker cell line were harvested by centrifugation at 1500*g* and resuspended in 100 μL of AMAXA Basic Parasite Solution 1. Then, after addition of 10 μg of the *NotI* linearized RNAi vector, transfection was performed with an AMAXA nucleofector II using program X-001. Immediately after transfection, cells were transferred to 30 mL of preincubated HMI-9 medium containing 5 μg/mL hygromycin, 2.5 μg/mL G418, and 2.5 μg/mL phleomycin. Serial dilutions of 1:10, 1:100, and 1:1000 were distributed to 24-well plates. Eight hours post transfection, puromycin was added to a final concentration of 0.3 μg/mL. Growth of transformed cultures was first observed 5 days post transfection and cultures derived from the 1:100 dilution expanded for further analysis. RNAi was induced by addition of 1 μg/mL tetracycline. Knockdown of topoisomerase II mRNA was confirmed by Northern blot analysis of RNA samples prepared from cells prior to and 24 h after induction of RNAi against topoisomerase II. Total RNA was prepared using the RNeasy kit (QIAGEN) and RNA samples were denatured with glyoxal and electrophoresis was performed on a vertical agarose gel. Blotting occurred by upward capillary transfer. The blot was probed using the DIG labeling sytem (Roche). DIG labeled DNA probes were generated for topoisomerase II (primers used for PCR amplification: 5′gcggaggcacacaagtat and 5′acgaggaaaactagaata, yielding a 1025 bp fragment) and for α-tubulin (primers used for PCR amplification: 5′cacttctatttatttatc and 5′gtcatcatggaggcgggc, yielding a 926 bp fragment). Hybridization was carried out overnight at 50 °C, and subsequent washes were performed at 42 °C. Topoisomerase II and tubulin mRNA, respectively, was detected after incubation with the chemiluminescence reagent CSPD (Roche).

In Vivo Activity against *T. brucei rhodesiense*.[44] Experiments in the *T. b. rhodesiense* (STIB900) acute mouse model were performed as preciously described,[44] with minor modifications. Briefly, female NMRI mice were infected interperitoneally (ip) with 10^4 *T. b. rhodesiense* bloodstream forms. Groups of four mice were treated perorally (po) with the compound, dissolved in a aqueous 1:1 dilution of the formulation (Cremophor RH40, Capmul MCM C8, triethylcitrate, ethanol), on days 3−6 post infection. A control group remained untreated. The parasitemia of all animals was checked every second day up to day 6 postinfection. Death of animals was recorded to calculate the mean survival time. Surviving and aparasitemic mice were considered cured at 60 days and then euthanized. All protocols and procedures used in the current study were reviewed and approved by the local veterinary authorities of the Canton Basel-Stadt, Switzerland.

■ ASSOCIATED CONTENT

Supporting Information

Further syntheses and spectroscopic data of all compounds, microanalysis, HPLC purities, logP values, and crystallographic data. This material is available free of charge via the Internet at http://pubs.acs.org.

■ AUTHOR INFORMATION

Corresponding Author

*Phone: 0931-31-85461. E-mail: holzgrab@pharmazie.uni-wuerzburg.de.

Notes

The authors declare no competing financial interest.

■ ACKNOWLEDGMENTS

We thank Elena Katzowitsch and Tobias Ölschläger (Institute for Molecular Infection Biology of the University of Würzburg) for the cytotoxicity screening, Jennifer Rath and Antje Fuss (Medical Mission Institute, Würzburg) for testing the compounds against *T. brucei brucei*, and the Deutsche Forschungsgemeinschaft (SFB 630) for financial support.

■ ABBREVIATIONS USED

BSF, bloodstream form; DAPI, 4′,6-diamidino-2-phenylindole; EMME, diethyl 2-(ethoxymethylene)-malonate; ER, endoplasmic reticulum; GFP, green fluorescent protein; HAT, human African trypanosomiasis; NMM, *N*-methylmorpholine; TDB, trypanosome dilution buffer; sulfo-NHS-AMCA, sulfosuccinimidyl-7-amino-4-methylcoumarin-3-acetate; YFP, yellow fluorescent protein

■ REFERENCES

(1) Cecchi, G.; Paone, M.; Franco, J. R.; Fevre, E. M.; Diarra, A.; Ruiz, J. A.; Mattioli, R. C.; Simarro, P. P. Towards the Atlas of human African trypanosomiasis. *Int. J. Health Geogr.* **2009**, *8*, 10.1186/1476-072X-8-15.

(2) *African Trypanosomiasis (Sleeping Sickness)*; World Health Organization Fact Sheet;World Health Organization: Geneva, 2006.

(3) Hide, G. History of sleeping sickness in East Africa. *Clin. Microbiol. Rev.* **1999**, *12*, 112−125.

(4) RaadtP.The history of sleeping sickness. Fourth International Cours on African Trypanosomoses, Tunis, Oct 11−28, 2005, World Health Organization: Geneva, 2005.

(5) Fèvre, E. M.; Wissmann, B.; Welburn, S. C.; Lutumba, P. The burden of human African trypanosomiasis. *PLoS Neglected Trop. Dis.* **2008**, 2 DOI: 10.1371/journal.pntd.0000333.

(6) Priotto, G.; Kasparian, S.; Mutombo, W.; Ngouama, D.; Ghorashian, S.; Arnold, U.; Ghabri, S.; Baudin, E.; Buard, V.; Kazadi-Kyanza, S.; Ilunga, M.; Mutangala, W.; Pohlig, G.; Schmid, C.; Karunakara, U.; Torreele, E.; Kande, V. Nifurtimox−eflornithine combination therapy for second-stage African *Trypanosoma brucei gambiense* trypanosomiasis: a multicentre, randomised, phase III, non-inferiority trial. *Lancet* **2009**, *374*, 56−64.

(7) Cavalli, A.; Bolognesi, M. L. Neglected tropical diseases: multi-target-directed ligands in the search for novel lead candidates against trypanosoma and leishmania. *J. Med. Chem.* **2009**, *52*, 7339−7359.

(8) (a) Cavalcanti, D. P.; Fragoso, S. P.; Goldenberg, S.; Souza, W.; Motta, M. C. M. The effect of topoisomerase II inhibitors on the kinetoplast ultrastructure. *Parasitol. Res.* **2004**, *94*, 439−448. (b) Kulikowicz, T.; Shapiro, T. A. Distinct genes encode type II topoisomerases for the nucleus and mitochondrion in the protozoan parasite *Trypanosoma brucei*. *J. Biol. Chem.* **2006**, *281*, 3048−3056.

(9) Sen, N.; Majumder, H. K. Mitochondrion of protozoan parasite emerges as potent therapeutic target: exciting drugs are on the horizon. *Curr. Pharm. Dis.* **2008**, *14*, 839−846.

(10) Lee, S. H.; Stephens, J. L.; Paul, K. S.; Englund, P. T. Fatty acid synthesis by elongases in trypanosomes. *Cell* **2006**, *126*, 691−699.

(11) Bodley, A. L.; Chakraborty, A. K.; Xie, S.; Burri, C.; Shapiro, T. A. An unusual type IB topoisomerase from African trypanosomes. *Proc. Natl. Acad. Sci. U.S.A.* **2003**, *100*, 7539−7544.

(12) Nenortas, E.; Burri, C.; Shapiro, T. A. Antitrypanosomal activity of fluoroquinolones. *Antimicrob. Agents Chemother.* **1999**, *43*, 2066−2068.

(13) Bringmann, G.; Hoerr, V.; Holzgrabe, U.; Stich, A. Antitrypanosomal naphthylisoquinoline alkaloids and related compounds. *Pharmazie* **2003**, *58*, 343−346.

(14) Nenortas, E.; Kulikowicz, T.; Burri, C.; Shapiro, T. A. Antitrypanosomal activities of fluoroquinolones with pyrrolidinyl substitutions. *Antimicrob. Agents Chemother.* **2003**, *47*, 3015−3017.

(15) Keiser, J.; Burri, C. Evaluation of quinolone derivatives for antitrypanosomal activity. *Trop. Med. Int. Health* **2001**, *6*, 369−389.

(16) Ma, X.; Zhou, W.; Brun, R. Synthesis, in vitro antitrypanosomal and antibacterial activity of phenoxy, phenylthio or benzyloxy substituted quinolones. *Bioorg. Med. Chem. Lett.* **2009**, *19*, 986−989.

(17) Gould, R. G.; Jacobs, W. A. The synthesis of certain substituted quinolines and 5, 6-benzoquinolines. *J. Med. Chem. Soc.* **1939**, *61*, 2890−2895.

(18) Shindikar, A. V.; Viswanathan, C. L. Novel fluoroquinolones: design, synthesis and in vivo activity in mice against Mycobacterium tuberculosis H37Rv. *Bioorg. Med. Chem. Lett.* **2005**, *15*, 1803−1806.

(19) Niedermeier, S.; Singethan, K.; Rohrer, S. G.; Matz, M.; Kossner, M.; Diederich, S.; Maisner, A.; Schmitz, J.; Hiltensperger, G.; Baumann, K.; Holzgrabe, U.; Schneider-Schaulies, J. A small-molecule inhibitor of Nipah virus envelope protein-mediated membrane fusion. *J. Med. Chem.* **2009**, *52*, 4257−4265.

(20) Koga, H.; Itoh, A.; Murayama, S.; Suzue, S.; Irikura, T. Structure−activity relationships of antibacterial 6,7- and 7,8-disubstituted 1-a1kyl-1,4-dihydro-4-oxoquinoline-3-carboxylic acids. *J. Med. Chem.* **1980**, *23*, 1358−1363.

(21) Heravi, M. M.; Jaddi, Z. S.; Oskooie, H. A.; Khaleghi, S.; Ghassemzadeh, M. Regioselective synthesis of quinolone antibacterials via borate complex of quinolone carboxylic acid. *J. Chem. Res.* **2005**, 578−579.

(22) Miyaura, M.; Suzuki, A. Palladium-catalyzed cross-coupling reactions of organoboron compounds. *Chem. Rev.* **1995**, *95*, 2457−2483.

(23) Austin, W. B.; Bilow, N.; Kelleghan, W. J.; Lau, K. S. Y. Facile synthesis of ethynylated benzoic acid derivatives and aromatic compounds via ethynyltrimethylsilane. *J. Org. Chem.* **1981**, *46*, 2280−2286.

(24) Gilligan, P. J.; Witty, M. J.; McGuirk, P. R. Substituted dihydroquinolone carboxylic acids, and antibacterial compositions containing them. Patent EP/184384/19860611, 1986.

(25) Vice, S.; Bara, T.; Bauer, A.; Fort, J.; Josien, H.; McCombie, S.; Miller, M.; Nazareno, A. P.; Tagat, J. Concise formation of 4-benzyl piperidines and related derivatives using a Suzuki protocol. *J. Org. Chem.* **2001**, *66*, 2487−2492.

(26) Räz, B.; Iten, M.; Grether-Bühler, Y.; Kaminsky, R.; Brun, R. The AlamarBlue assay to determine drug sensitivity of African trypanosomes (*T. brucei rhodesiense* and *T. brucei gambiense*) in vitro. *Acta Trop.* **1997**, *68*, 139−147.

(27) Baltz, T.; Baltz, D.; Giroud, C.; Crocket, J. Cultivation in a semi-defined medium of animal infective forms of *Trypanosoma brucei*, *T. equiperdum*, *T. evansi*, *T. rhodesiense* and *T. gambiense*. *EMBO J.* **1985**, *4*, 1273−1277.

(28) Ahmed, S. A.; Gogal, R. M.; Walsh, J. E. A new rapid and simple non-radioactive assay to monitor and determine the proliferation of lymphocytes: an alternative to [^{3}H]thymidine incorporation assay. *J. Immunol. Methods* **1994**, *170*, 211−224.

(29) Alptüzün, V.; Prinz, M.; Hörr, V.; Scheiber, J.; Radacki, K.; Fallarero, A.; Vuorela, P.; Engels, B.; Braunschweig, H.; Erciyas, E.; Holzgrabe, U. Interaction of (benzylidene-hydrazono)-1,4-dihydropyridines with β-amyloid, acetylcholine, and butyrylcholine esterases. *Bioorg. Med. Chem.* **2010**, *18*, 2049−2059.

(30) Lipinski, C. A.; Lombard, F.; Dominy, B. W.; Feeney, P. J. Experimental and computational approaches to estimate solubility and permeability in drug discovery and development settings. *Adv. Drug Delivery Rev.* **2001**, *46*, 3−26.
(31) Tenjarla, S. Microemulsions: an overview and pharmaceutical applications. *Crit. Rev. Ther. Drug Carrier Syst.* **1999**, *16*, 461−521.
(32) Date, A. A.; Nagarsnker, M. S. Parenteral microemulsions: an overview. *Int. J. Pharm.* **2008**, *355*, 19−30.
(33) Benita, S. Submicron Emulsion in Drug Targeting and Delivery; Harwood Academic Publishers: Amsterdam, 1998.
(34) Wang, Z.; Englund, P. T. RNA interference of a trypanosome topoisomerase II causes progressive loss of mitochondrial DNA. *EMBO J.* **2001**, *20*, 4674−4683.
(35) Lindsay, M. E.; Gluenz, E.; Gull, K.; Englund, P. T. A new function of *Trypanosoma brucei* mitochondrial topoisomerase II is to maintain kinetoplast DNA network topology. *Mol. Microbiol.* **2008**, *70*, 1465−1476.
(36) Wohlkonig, A.; Chan, P. F.; Fosberry, A. P.; Homes, P.; Huang, J.; Kranz, M.; Leydon, V. R.; Miles, T. J.; Pearson, N. D.; Perera, R. L.; Shillings, A. J.; Gwynn, M. N.; Bax, B. D. Structural basis of quinolone inhibition of type IIA topoisomerases and target-mediated resistance. *Nature Struct. Mol. Biol.* **2010**, *17*, 1152−1153.
(37) Hansch, C.; Leo, A.; Hoekman, D. *Exploring QSAR: Volume 2: Hydrophobic, Electronic and Steric Constants*; American Chemical Society: Waschington DC, 1995.
(38) Clarke, J.; Cunliffe, A. E. Rapid spectrophotometric measurement of ionisation constants in aqueous solution. *Chem. Ind. (London)* **1973**, 281.
(39) Albert, A.; Serjeant, E. P. Ionisation constants of acids and bases. Wiley Inc.: New York, 1962.
(40) Box, K.; Comer, J. E.; Gravestock, T.; Stuart, M. New ideas about the solubility of drugs. *Chem. Biodiversity* **2009**, *6*, 1767−1788.
(41) Rasband, W. S. *ImageJ*; National Institutes of Health: Bethesda, MD, 1997−2008; http://rsb.info.nih.gov/ij/.
(42) Strauss, P. R.; Wang, J. C. The TOP2 gene of *Trypanosoma brucei*: a single-copy gene that shares extensive homology with other TOP2 genes encoding eukaryotic DNA topoisomerase II. *Mol. Biochem. Parasitol.* **1990**, *38*, 141−150.
(43) Wickstead, B.; Ersfeld, K.; Gull, K. Targeting of a tetracycline-inducible expression system to the transcriptionally silent minichromosomes of *Trypanosoma brucei*. *Mol. Biochem. Parasitol.* **2002**, *125*, 211−216.
(44) Kaiser, M.; Bray, M. A.; Cal, M.; Bourdin Trunz, B.; Torreele, E.; Brun, R. Antitrypanosomal activity of fexinidazole, a new oral nitroimidazole drug candidate for treatment of sleeping sickness. *Antimicrob. Agents Chemother.* **2011**, *55* (12), 5602−5608.